International Journal of Innovative Computing, Information and Control
Volume **19**, Number **6**, December **2023**

ICIC International ©2023 ISSN 1349-4198
pp. 1953–1968

FAULT DIAGNOSIS METHOD OF MIGRATION LEARNING BASED ON ANTAGONISM GENERATION NETWORK

Jie Sun*, Yan Wang, Yi Sun and Fangming Jin

Qiqihar Power Supply Branch of State Grid Heilongjiang Electric Power Co., Ltd.
No. 288, South Road, Longsha District, Qiqihar 161005, P. R. China
{ hljlibing; xtchenyan }@yeah.net; jinfangming2023@126.com
*Corresponding author: qhdgaoyh@163.com

Received March 2023; revised July 2023

Abstract. *Intelligence and automation technology are key to promoting the development of modern industrial manufacturing; therefore, ensuring the safe and effective operation of motors is an important research topic. Introducing deep learning technology into the fault diagnosis environment of motor systems, considering the nonlinear characteristics of industrial mechanical system signals, it is difficult to effectively obtain mechanical data signals. Therefore, the transfer learning of the physical diagnosis model is studied, the traditional confrontation generation network is optimized, and the collected real features are integrated into the physical model to build the mechanical fault diagnosis model of the boundary balanced confrontation generation network (Boundary Equilibrium GAN, BEGAN). At the same time, because the BEGAN model is faced with the problem of declining correlation of generated data, transfer learning is introduced to optimize the fault diagnosis model. Input the collected common motor fault data into the fault diagnosis model for training, improve the model's fault diagnosis accuracy, and thus achieve effective diagnosis of motor faults. In the test of motor bearing simulation spectrum diagram, the motor health, outer ring fault and inner ring fault meet the requirements of simulation vibration signal sequence, and the amplitude is $A_0 > A_i > A_H$. The typical KNN and K-means algorithm are selected for comparison with the proposed FD model. In the FD of outer circle, the correct rate of FD of the proposed method is 0.923, which is higher than 0.815 and 0.885 of KNN and K-means. The diagnosis effect of the Fault Detection (FD) model is excellent and meets the needs of mechanical FD. The innovative application of machine learning technology in the field of motor faults through diagnostic model training and recognition of motor health status has important reference value for improving the effectiveness of industrial machinery fault diagnosis.*
Keywords: BEGAN, Transfer learning, Motor fault, Diagnosis, Test

1. **Introduction.** In the field of modern industrial manufacturing, motors are very important automation equipment. With the improvement of software and hardware technology, the motor system is developing towards high efficiency, integration and large scale. Therefore, the internal structure of industrial motor is more precise and complex. For the motor with high load operation, once the fault occurs, it brings serious challenges to the production and safety of the enterprise. Ensuring stable operation of motor equipment is a difficult problem for enterprises at present. The health detection and fault diagnosis of industrial electromechanical equipment has become one of the core technologies of intelligent manufacturing. Modern industrial equipment generally has high integration and a large number of electronic precision parts. The application of high-precision instruments and equipment increases the diagnostic requirements of motor equipment. At present, the health detection of industrial electromechanical equipment usually relies on

DOI: 10.24507/ijicic.19.06.1953

the internal sensor detection data of motor equipment, including internal vibration data, noise parameters, etc., to diagnose mechanical faults through the judgment of abnormal data information. Obviously, traditional fault diagnosis methods cannot meet the current diagnostic needs of electrical machinery. In recent years, computer communication and other technologies have been integrated into the field of industrial manufacturing, and through real-time monitoring and massive data storage, different status data of mechanical equipment can be effectively collected. The integration of data-driven and machine learning technology in mechanical fault diagnosis greatly improves the diagnostic effectiveness of motor faults. Therefore, deep learning technology is introduced into the diagnosis of industrial motor faults. By analyzing the characteristics of motor diagnostic data and utilizing intelligent machine learning models to analyze motor fault information, a motor fault diagnosis model based on deep learning is constructed. The improved diagnosis model improves the shortcomings of traditional fault detection technology data recognition, and obtains more accurate diagnostic data through model training to ensure the safe and stable movement of industrial motors. It has important reference value for the development of industrial intelligence and automation.

2. **Related Work.** In the field of industrial manufacturing, mechanical fault is one of the main problems faced by enterprises. Due to the continuous innovation of information industry technology, intelligent FD technology has been developed, and relevant scholars at home and abroad have done massive research on this area. Li and others found that industrial IoT technology has been widely used in manufacturing environment. It was difficult to detect mechanical equipment under different working conditions in fault diagnosis. An optimized adaptive FD scheme was proposed. The maximum average difference and domain antagonism training were used to identify and judge features, so as to obtain accurate FD results. The findings showed that the proposed scheme had good diagnostic effect in mechanical FD [1]. Guo et al. carried out research on mechanical FD and found that data drive was crucial to the safety and stability of equipment. An FD framework was proposed. In this framework, auxiliary classifiers were preferentially used to generate real damage data. At the same time, the damage data and real data were trained and classified to achieve effective detection of equipment faults. The proposed method greatly improved the fault detection accuracy [2]. Li et al. found that intelligent FD technology based on depth technology has been largely adopted in many areas. There is a good solution to the problem of sharing related faults between the source domain and the target domain. Considering the particularity and complexity of mechanical fault, a fault detection method for motor equipment was proposed. This method used adversarial learning to build a learning model to identify and classify fault types. Then an automatic encoder model with silhouette coefficient was established to sort out the fault types. The findings showed that this method had higher diagnostic accuracy than traditional diagnostic model [3]. Shao et al. studied the rotor-bearing FD strategy and found that the existing diagnosis technology was not suitable for the situation. Therefore, a new FD model of rotor bearing system was built based on improved convolution network. It indicated that the scheme had wider adaptability and higher FD ability [4].

In recent years, machine learning and other technologies have been largely adopted in the field of mechanical fault diagnosis, significantly improving the health diagnosis effect of industrial equipment. Abubakar et al. studied motor fault types and proposed a new enhanced model for motor FD based on adaptive system. The performance experiment showed that the method had good robustness and diagnosis effect [5]. Chen et al. carried out research on deep learning technology used in the field of mechanical FD and found that deep learning had excellent performance in fault diagnosis. An improved learning model based on neural network was proposed. Firstly, a one-dimensional convolution was constructed based on the task data set, and the transfer learning strategy was used to complete the depth model training task. The method was applied to four typical fault case environments, and the proposed scheme had good FD ability [6]. Jiao et al. studied the problem of mechanical fault diagnosis. Due to the internal complexity of mechanical equipment, changes in internal and external data of equipment affect the results of FD and reduce the accuracy of fault diagnosis. To solve this problem, an unsupervised intelligent diagnosis method was constructed. This method was based on the antagonism adaptive network and realized classification of data in different test areas. To verify the effect of the proposed method, 15 typical diagnostic tasks were built. It turned out that the proposed FD method has more comprehensive effect [7].

According to the above research, mechanical FD technology has developed rapidly. The application of deep learning and other technologies in the field of mechanical fault diagnosis effectively solves the limitations of traditional equipment fault diagnosis techniques. However, the application of deep learning technology in the field of fault diagnosis requires a large amount of learning data, and a large number of data sources need to be collected to improve the training accuracy of the model. Therefore, the FD model based on deep learning technology can provide effective reference for the development of intelligent industry.

3. Construction of Migration Learning FD Model Based on Confrontation Generation Network.

3.1. Construction of FD model based on confrontation generation network.

Due to the high integration and complex internal structure of modern industrial motor equipment, it is difficult to collect and label the signal of fault problems and effectively diagnose the equipment fault problems. Therefore, starting from the physical model of the motor, the model simulation fault data is analyzed. The matching signal is generated by the confrontation network and the mechanical FD is completed by the classifier [8]. In the study of the physical model of the motor, the dynamic parameters of the model can effectively reflect the internal working conditions of the machine. The research mainly adopts the mixed parameter method to adjust the internal parameters of the machine. The system layer of motor mechanical structure is divided into rolling body, inner ring, shaft, outer ring and other parts. The system can be simplified as an elastic-mass-damping system. Figure 1 shows the hybrid structure of the motor.

In Figure 1, the outer ring of motor bearing is mainly fixed on the plane by damping equipment. In actual operation, the motor uses mass elasticity to reflect the operation status of the whole system. The operation of motor system is represented by physical model, as shown in Formula (1) [9].

$$m\ddot{x} = \sum F \tag{1}$$

In Formula (1), $\sum F$ represents the total external force of the mechanical action on the object. m is the mass parameter of the machine. $\ddot{x}$ represents mechanical vibration acceleration. The quasi-static state of motor equipment is studied. In the mechanical model, the force and torque in the machine are in a static state. At this moment, the state of the model is shown in Formula (2).

$$\begin{cases} \sum F = 0 \\ \sum M = 0 \end{cases} \tag{2}$$

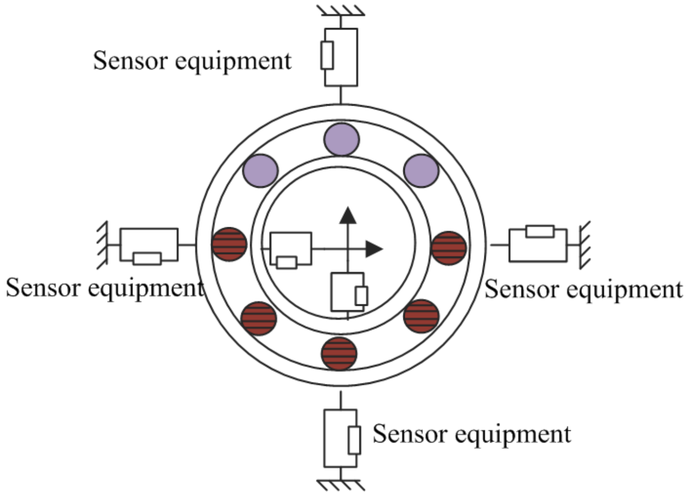

FIGURE 1. Internal mixed parameter structure of motor

In Formula (2), M represents torque. $\sum M$ is torque sum. In the quasi-dynamic state, except for the torque, the mechanical interior is in the force balance state. The state expression is shown in Formula (3).

$$\begin{cases} \sum F = 0 \\ \sum M = J\dot{\omega} \end{cases} \tag{3}$$

In Formula (3), J represents the moment of inertia. $\dot{\omega}$ is the frequency of mechanical unbalance vibration. If the machinery is abnormal, the internal force and torque are in an unbalanced state, as shown in Formula (4) [10].

$$\begin{cases} \sum F = \ddot{x}m \\ \sum M = J\dot{\omega} \end{cases} \tag{4}$$

Through the analysis of the internal state parameters of the motor, the operation status of the internal system of the motor can be reflected. However, it is difficult to obtain useful motor fault information only relying on the physical model parameters of the motor [11]. Therefore, the physical model parameters are considered to be converted into fault simulation signals. The more accurate FD data can be obtained by constructing the confrontation generation model through the recognizer and generator. The confrontation generation model is an unsupervised neural network, which can learn the data distribution and complete the sampling operation [12]. The confrontation generation model is mainly composed of generators and recognizers. The structure flow is shown in Figure 2.

In the Generic Adversarian Network (GAN), the generator is mainly used to generate similar distributed data, while the recognizer is mainly used to identify and judge the data sources [13]. The recognizer target is shown in Formula (5).

$$\max_G V(G,D) = E_{G(n)-P_{GD}}[-\log(1-D(D(n)))] + E_{x-P_{RD}}[-\log(D(x))] \tag{5}$$

In Formula (5), $G(n)$ is generator. $D(x)$ represents recognizer. n is input. P_{GD} indicates generated distribution data. The generator target expression is shown in Formula (6).

$$\min_D V(G,D) = E_{G(n)-P_{GD}}[-\log(1-D(D(n)))] + E_{x-P_{RD}}[-\log(D(x))] \tag{6}$$

The goal of GAN model is shown in Formula (7).

$$V(G,D) = -\int P_{GD}(x)\cdot(-\log(1-D(x))) + P_{RD}(x)\cdot(\log(D(x)))dx \tag{7}$$

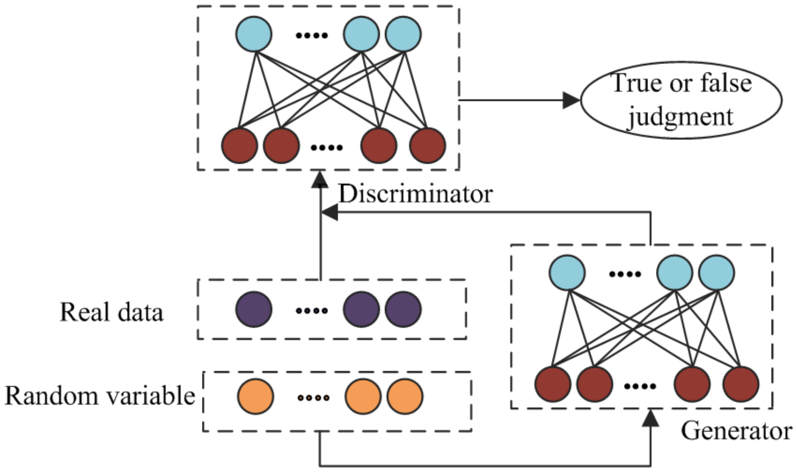

FIGURE 2. Flow diagram of GAN model

When the optimal solution is obtained in Formula (7), the expression of $D(x)$ is shown in Formula (8).

$$D(x) = \frac{P_{RD}(x)}{R_{RD}(x) + P_{GD}(x)} \tag{8}$$

In model training, only when the generated distribution data is consistent with the real distribution data can the model obtain the optimal solution. However, the confrontation generation model is prone to fall into local convergence in actual training, which affects the actual training effect [14]. At the same time, it is difficult to maintain the balance between the recognizer and generator in the model, which makes it difficult to achieve the optimal effect of model training. Therefore, boundary confrontation generation network (BEGAN) is used to solve the above problems. Figure 3 depicts the flow structure of BEGAN model [15].

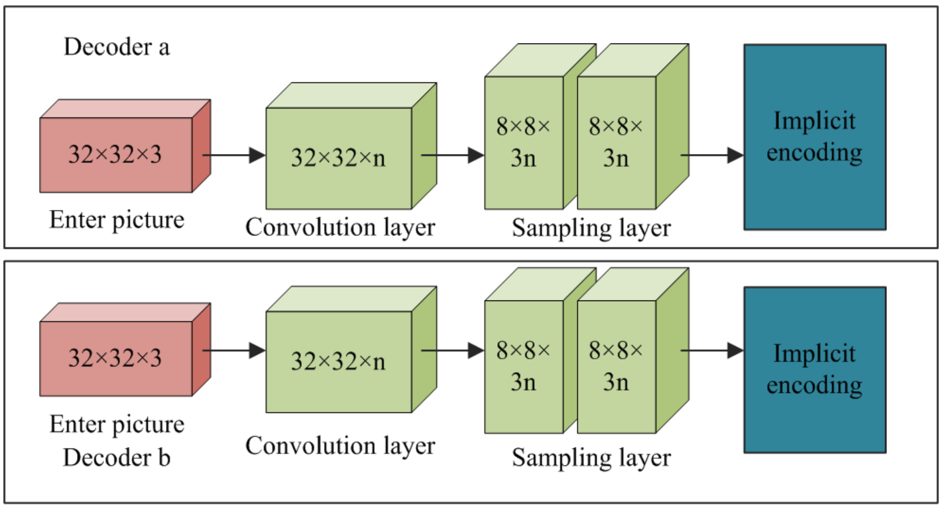

FIGURE 3. Flow structure of BEGAN model

The BEGAN model contains an implicit code to generate a two-dimensional map of the map, which can be used with the recognizer to determine whether the image is true or false. W is the distance between the source domain and the generated domain, as shown in Formula (9).

$$W(\mu_1, \mu_2) = \inf_{\gamma \in \Gamma(\mu_1, \mu_2)} E_{(x_1, x_2) - \gamma} |x_1 - x_2| \tag{9}$$

In Formula (9), x_1 and x_2 represent the two loss function values of $\gamma = (\mu_1, \mu_2)$. γ represents the parameter exceeding the limit. μ_1 and μ_2 are two distribution functions of reconstruction. In the BEGAN model, the operation principle is not to directly optimize the lower boundary of Wasserstein Distance (LWD). In model training, a good self-coder can correctly decode and complete data distribution sampling in the source domain, and ensure that the coding loss of model training tends to 0 [16]. When the input data does not meet the requirements of source domain distribution, the coding loss during model training is larger. Therefore, the BEGAN model can judge the signal distribution between each domain by the coding loss, and cannot directly optimize the coding loss. Therefore, the inequality transformation is used as shown in Formula (10).

$$\inf E[|x_1 - x_2|] \geq \inf |E[x_1 - x_2]| = |m_1 - m_2| \tag{10}$$

In Formula (10), $|m_1 - m_2|$ represents the lower bound of distance. μ_1 is $L(x)$ distribution. μ_2 and μ_1 are $G(z)$ distributions. Because the real distribution of the original GAN model is similar to the generated distribution, it increases the difficulty of model training when $m_1 = m_2$. Therefore, the over-standard parameter γ is defined in interval $[0, 1]$ to avoid the occurrence of $m_1 = m_2$. The final goal of the BEGAN model is equilibrium, so the target parameters are expressed as shown in Formula (11).

$$M_{global} = L(x) + |\gamma L(x) - L(G(Z_G))| \tag{11}$$

In Formula (11), Z_G represents GAN original generated data. M_{global} is the training degree of the model. The higher the M_{global} value, the better the training effect of the model.

3.2. **Construction of transfer learning FD model based on physical model.** Due to the large number of diagnostic datasets involved in the detection of motor systems, and the tendency to overlook the correlation between generator input and output data in BEGAN model training, motor operation generates a large amount of signal data, which requires huge storage and computing power. Strong computing power is very expensive. In addition, the training of massive data requires a lot of time, leading to the contradiction between big data and weak computing. Through transfer learning, the quality and quantity of training data can be improved. At the same time, most of the data in transfer learning are trained in other source domains before the trained model is transferred to the target domain, which greatly reduces the computational requirements of the training process in the target domain and improves the diagnostic effect of the model. Therefore, transfer learning is introduced to optimize this problem, and DABEGAN fault diagnosis model is constructed. Figure 4 shows flow structure of the improved DABEGAN model [17].

In the DABEGAN FD model, two identical self encoders are added. Figure 4 depicts the details. The diagnosis signal generated by the mechanical model of the motor is transferred to the generator in the model training. The generator processes the unlabeled real signal and the generated signal, and the two signals complete the training together in the recognizer. The recognizer judges the true and false of the two signals in training, so that the collected signals are consistent with the generated signals, and meet the requirements of adding true features in the simulation signals. Finally, the FD signal classification results are obtained by using the distributed signals with labels and the real signals, so as to achieve effective classification of mechanical faults [18]. In the DABEGAN model, there are two self encoders with the same structure to form the recognizer and generator. They contain six layers of convolution. The self encoder structure is shown in Figure 5.

In Figure 5, self-coding includes identifying and generating two encoders. The structure is composed of multiple 2D Cov2D convolution layers. The convolved graph contains

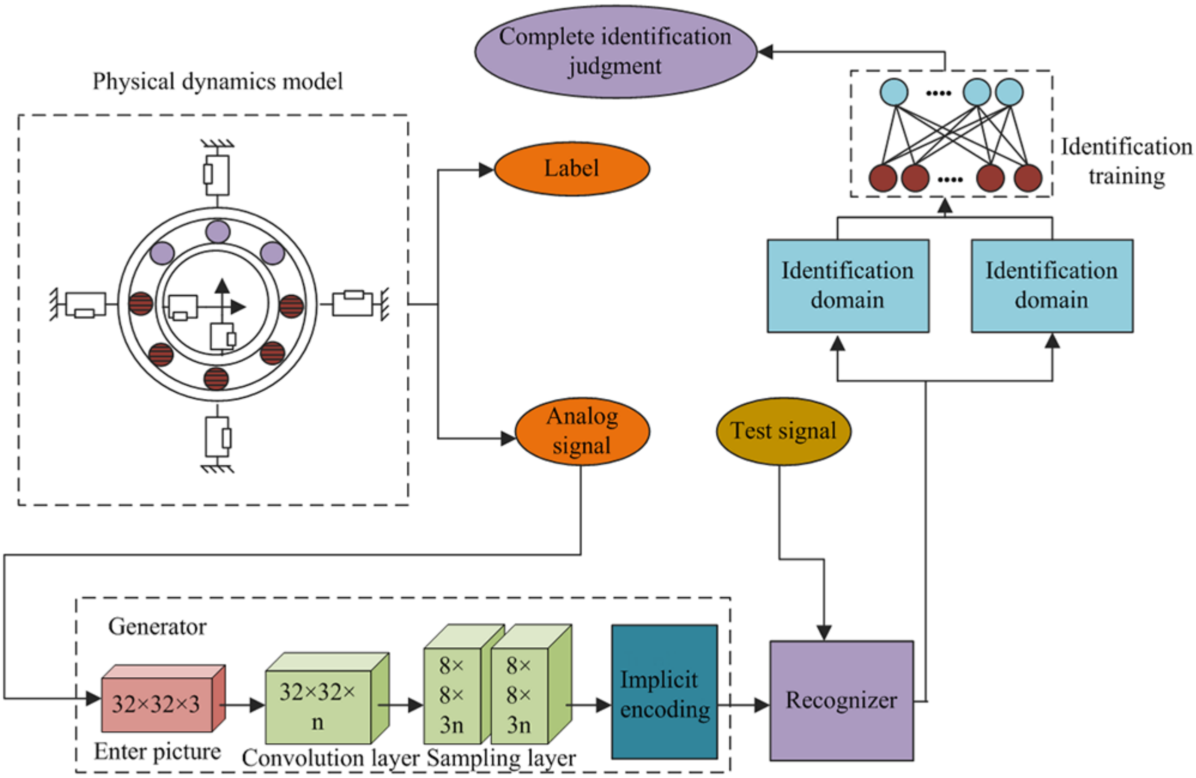

FIGURE 4. Flow structure of improved DABEGAN model

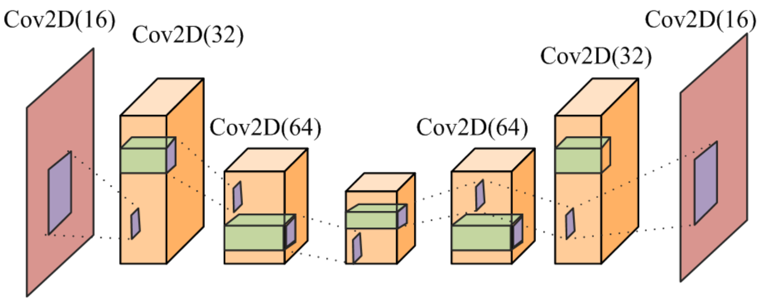

FIGURE 5. Schematic diagram of self-coding structure

multiple channels, and the size of each channel is $y \times z$. The normalized output characteristics are required after the convolution processing. Leaky ReLu is selected as the activation function in the study, and the expression is shown in Formula (12).

$$y = \max(0, x) + a \cdot \min(0, x) \tag{12}$$

In Formula (12), the value of a is 0.01. The proposed DABEGAN model has excellent domain adaptability. In source domain signal processing, the classifier can generate generated signals similar to target domain distribution more quickly. There is a problem of signal migration in the training of the DABEGAN model. The probability distribution of high-dimensional data features can be processed by different projection surfaces to obtain the low-dimensional data feature distribution. However, when high-dimensional features are processed to low-dimensional features, the data features show similar distribution. The distribution after low-dimensional processing is shown in Figure 6 [19].

Different characteristics belong to different types. The similarity distribution causes problems in feature mapping. To overcome this problem, although regularization can

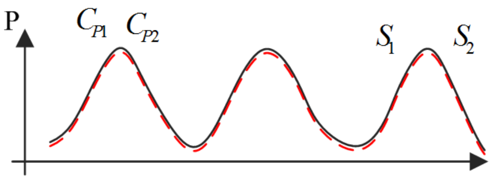

FIGURE 6. Distribution after low-dimensional processing

be used to constrain the change of the generation domain and the source domain, the self-adaptability of the BEGAN model domain is significantly limited, which affects the distribution of the generated feature data. Therefore, a boundary constraint is added between the target domain signal n and the generated signal $G(n)$ of the diagnostic model to solve this problem, as shown in Formula (13) [20].

$$L_{gt}(n) = |G(n) - n| \tag{13}$$

In Formula (13), $L_{gt}(n)$ represents the constraint limit. After adding constraints to the model, the generator closes to the same target in the source domain when generating data, but the signal is far away from the target domain. The graph loss after being constrained is shown in Formula (14).

$$L_g(n) = |Mean(G(n)) - Mean(n)| \tag{14}$$

In Formula (14), $Mean(\cdot)$ represents the mean function. The input of the average root value is shown in Formula (15).

$$Mean(x) = \frac{\sum_{X \in x} x}{N} \tag{15}$$

From Formula (13) to Formula (15), the total target of the generator is shown in Formula (16).

$$L_{G1}(n, \theta_G) = Mean(L_A(G(n)) + L_G(n)) \tag{16}$$

In Formula (16), θ_G is the generator parameter. $L(\cdot)$ is the coding loss function. The problem of data signal migration can be solved through the above constraints.

4. FD Model Simulation Test.

4.1. Motor physical model simulation signal test. Industrial manufacturing large motor equipment is selected as the FD object, and judge whether the motor is faulty based on the vibration of the motor bearing. The motor bearing signal is mainly collected by the internal sensor of the motor. The fault model of the inner and outer rings of the motor is shown in Figure 7.

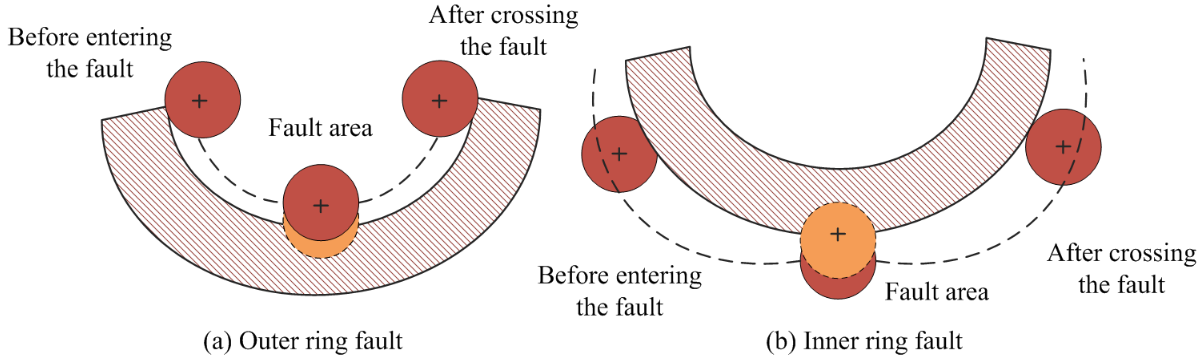

FIGURE 7. Motor fault type

Figure 7 shows the fault types of the outer and inner rings of the motor bearing. Affected by internal and external factors, the rolling element inside the motor enters the fault area and increases the distance between the bearing and the rolling element. At this moment, the force on the rolling element entering the fault area rapidly decreases and expands the radial indirection. Two types of fault data of the motor can be obtained from the sensor, and then the dynamic model of the motor can be constructed. The Runge-Kutta method is used to solve the motor signal simulation results, as shown in Figure 8.

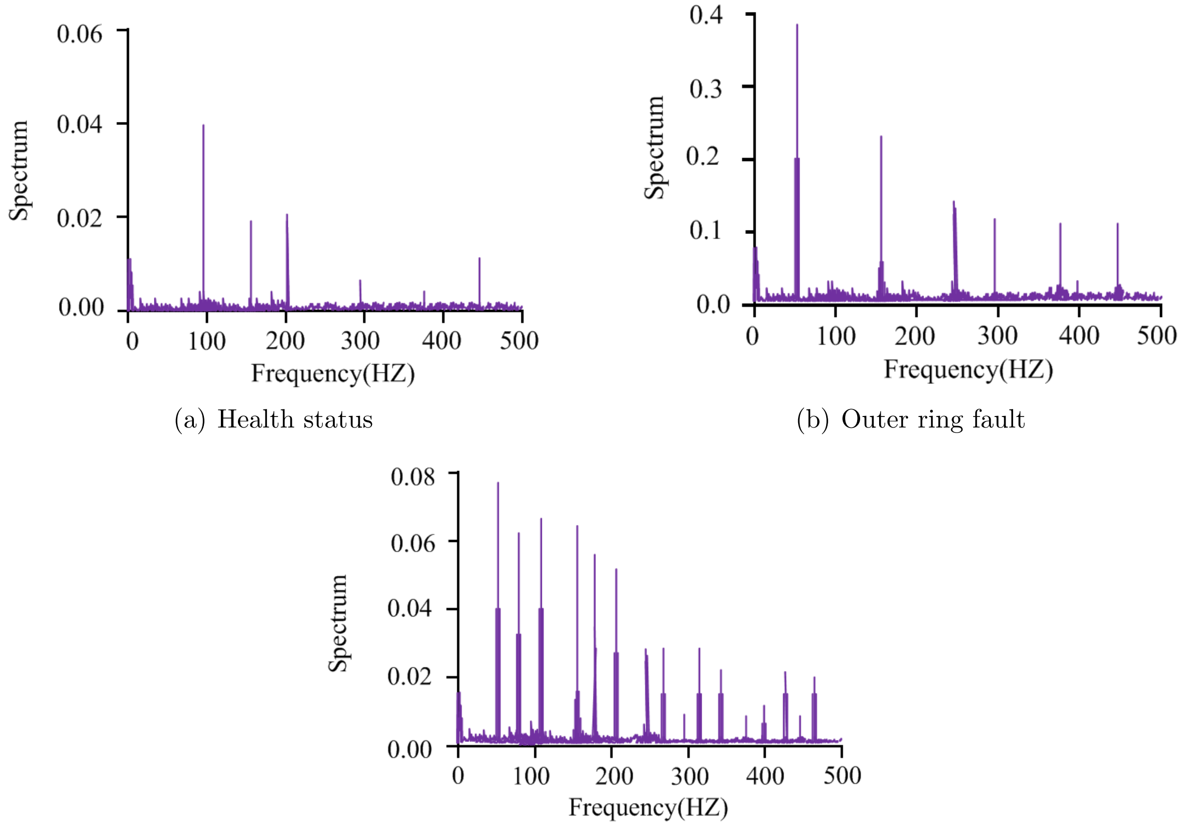

(a) Health status

(b) Outer ring fault

(c) Inner ring fault

FIGURE 8. Simulation spectrum of motor bearing

Figure 8(a), Figure 8(b) and Figure 8(c) show the simulation signal diagrams of motor health, outer ring fault and inner ring fault, respectively. The simulated vibration signal of the motor meets the $A_0 > A_i > A_H$ sequence requirements. Among them, A_0 is the outer circle fault amplitude signal, A_i is the inner circle fault amplitude signal, and A_H is the health amplitude signal. Because the physical model is affected by noise in fault signal detection, there are some abnormal curves in the actual spectrum. In the motor fault monitoring, the motion frequency of the rolling element is consistent with the fault frequency, so the amplitude is also consistent. However, the increase of the outer ring A_0 may be caused by debris or lubrication in the motor. In the healthy state, the low-frequency signal is interfered by noise factors. The real signal and the simulated signal have a large difference. Only relying on the results of mechanical internal simulation signals cannot accurately determine the type of motor fault. Therefore, the simulation information is taken as the fault feature test sample. The proposed FD model is used for further mechanical fault diagnosis.

4.2. **Performance test of FD model.** To test the effect of the FD in motor fault diagnosis, the Windows 10 system platform is selected as experiment platform. The processor is INTEL i7 64-core, and the graphics card is NVIDIA RTX30370. The performance test of the diagnosis model is completed based on TensorFlow 1.4 learning platform. 1200 common motor fault data are collected as model test samples. The model learning rate is set to 0.0001, and the model batch training size is 100. Figure 9 shows the test results using the proposed BEGAN FD model.

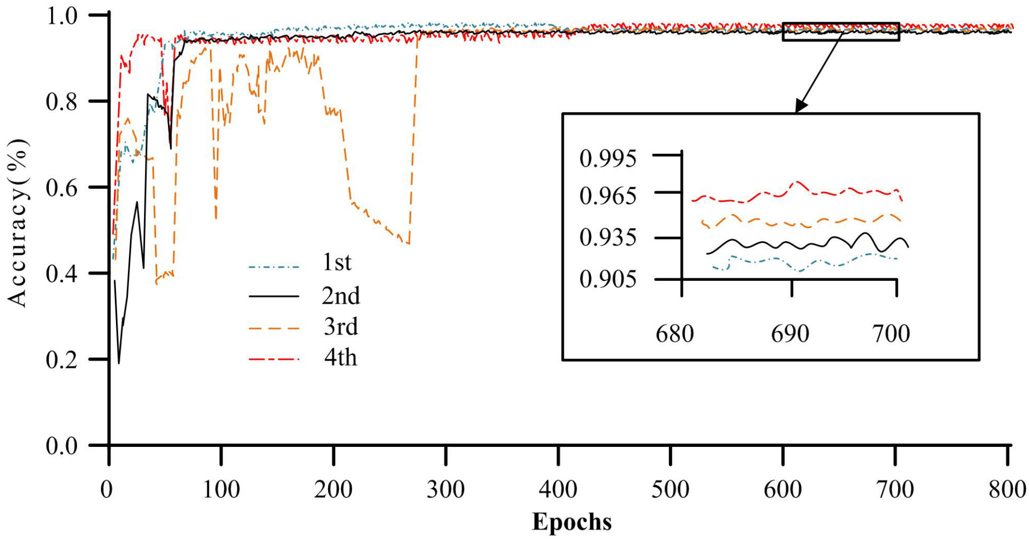

Figure 9. Multiple training results of the proposed fault diagnosis model

Figure 9 shows the FD results of multiple training of the proposed model. The proposed FD model combines the transfer learning theory and has good domain adaptive ability. However, GAN model is easy to fall into local convergence in training, which affects the recognition training effect. Therefore, to test the reproducibility of the diagnosis model, the optimized diagnosis model is tested repeatedly. From Figure 9, the accuracy rate of FD for the four training sessions has exceeded 0.905, indicating that the FD has good diagnostic ability. However, in the first test and the second test, the model stability is poor, and there is a large curve fluctuation in the early training. By analyzing the curve of the previous test, the generator is relatively fragile in the initialization stage of the model training, which affects the performance of the model and causes large recognition losses. The difference between the source domain signal and the generated signal also affects the model mapping effect. Therefore, the model has a large curve fluctuation in the first test and the second test. After many tests, the error of the model gradually decreases, thus improving the accuracy and stability in the early training. To test whether the optimized method can reduce the model training mapping error, the original BEGAN model with generator regular term removed is tested by experimental simulation. The FD results of the original BEGAN model are shown in Figure 10.

Figure 10 shows the results of three repeated training tests of the original fault diagnosis model. According to the test curve in the figure, compared with the improved fault diagnosis model, the overall training accuracy of the original BEGAN fault diagnosis model is poor, and there are significant fluctuations in the training curve during testing, indicating that the training stability of the original BEGAN model is poor. The average diagnostic accuracy of the original BEGAN fault diagnosis model was 0.435 for the first time, 0.664 for the second time, and 0.675 for the third time. Compared with the test results in Figure 9, the proposed improved DABEGAN fault diagnosis model has an improvement of 36.5%

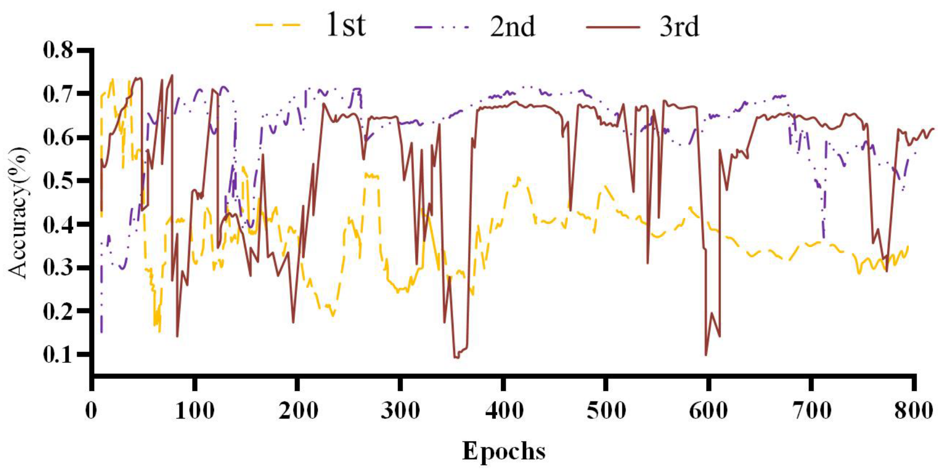

FIGURE 10. Results of multiple training tests of the original BEGAN fault diagnosis model

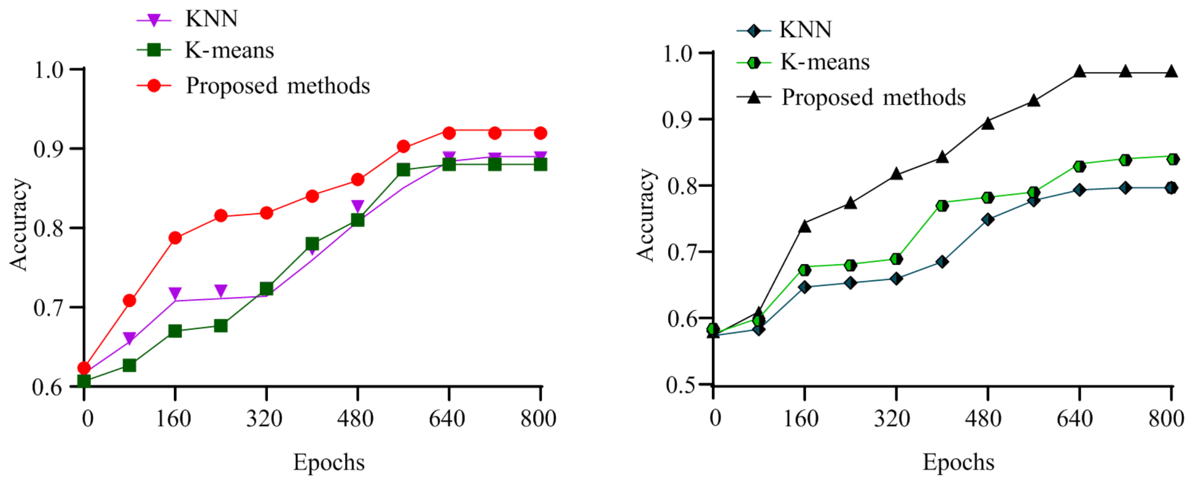

(a) Outer ring fault (b) Inner ring fault

FIGURE 11. Training and test results of various fault diagnosis models

compared to the original BEGAN, indicating that the proposed diagnostic model reduces the mapping error during model training and also has superior domain adaptability. In order to compare the performance of the proposed fault diagnosis model, a typical neighbor algorithm (KNN, K-Nearest Neighbor) and a clustering algorithm (K-means clustering algorithm) were selected to participate in the model performance test. The test results are shown in Figure 11.

Figure 11 shows the mechanical FD results of three FD models. Figure 11(a) shows the FD test results of the motor outer ring. From the figure data, the three FD models have obvious differences. The overall test performance of K-means FD model is the worst. After 640 iterations, it tends to converge. The FD accuracy of K-means model is 0.885. Next is the KNN FD model, which tends to converge after 710 iterations. The accuracy is 0.815. The best performance is the model proposed by the research. According to the model training curve, the proposed model tends to converge after 640 iterations, and the FD accuracy is 0.923. The proposed FD model has the best FD accuracy and faster convergence effect. Figure 11(b) shows the FD test results of the inner ring of the motor. According to the results of model training curve, the proposed FD model is the best of the three FD models. It tends to converge after iteration 632. The FD accuracy of the model is 0.986. The second is K-means FD model, which tends to converge after 672 iterations, and the FD accuracy is 0.876. The KNN FD model with the worst performance tends to converge after iteration 710, and the FD accuracy is 0.801. Compared with the outer circle FD results, the inner circle FD accuracy is significantly higher, mainly because the outer circle fault factors are more complex. The proposed FD model has excellent iterative performance and FD accuracy. At the same time, select the outer circle data to verify the model test effect, and conduct t test on the K-means model and the proposed method, as shown in Table 1.

Table 1. Model training data verification results

Group	Iteration 160	Iteration 320	Iteration 480
K-means (accuracy)	0.712	0.726	0.826
Proposed method (accuracy)	0.823	0.843	0.886
t value	2.466	2.056	1.656
p value	< 0.05	< 0.05	< 0.05

From the results in Table 1, it can be seen that during 160 iterations, the K-means model was 0.712, and the accuracy of the proposed model was 0.823. There was a significant difference between the two groups of data ($p < 0.05$). At 320 iterations, the K-means model was 0.726, and the accuracy of the proposed model was 0.843. There was a significant difference ($p < 0.05$) between the two sets of data. At 480 iterations, the K-means model was 0.826, and the accuracy of the proposed model was 0.886. There was a significant difference in comparison between the two sets of data ($p < 0.05$). It can be seen that the proposed model has a significant difference in effectiveness compared to traditional diagnostic models, and the proposed model has better diagnostic performance. Finally, visualize and compare the images generated by the proposed fault diagnosis model, as shown in Figure 12.

Figure 12 shows the result of visual features generated by the proposed model. The triangular part is the health feature, the diamond part is the inner ring fault feature, and the circular part is the outer ring fault feature. Figure 12(a) shows the visual characteristic image of the generated domain, Figure 12(b) shows the visual characteristic image of the recognition generated domain, and Figure 12(c) shows the visual characteristic image of the target domain. Figure 12(a), Figure 12(b) and Figure 12(c) clearly show the richness of sample features. The richer the sample features are, the more difficult it is to classify them in fault diagnosis. Figure 12(d) shows a visual feature image of recognition target domain. Compared with Figure 12(c), the coverage status of different types of FD features has decreased, and the distribution of different features is denser. In Figure 12(c), a large number of health features are distributed around the outer circle fault features and the inner circle fault features, which increases the difficulty of feature recognition and classification. In Figure 12(d), the generator and recognizer in the model can migrate from the source domain to the target domain. Figure 12(e) shows the source domain visualization feature image. The fault feature distribution in Figure 12(e) is different from that in Figure 12(c) and Figure 12(d). Therefore, in the model training test, the generation domain is similar to the target domain feature signal, and the recognition generation domain is the same as the recognition target domain signal feature.

Through this recognition principle, the characteristics of mechanical faults can be identified more accurately, thus improving the overall diagnosis effect of mechanical faults.

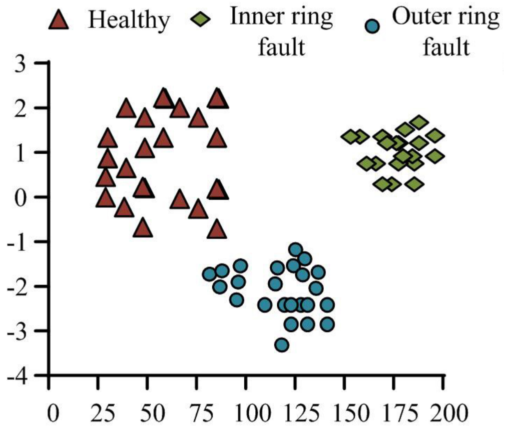

(a) Generated domain

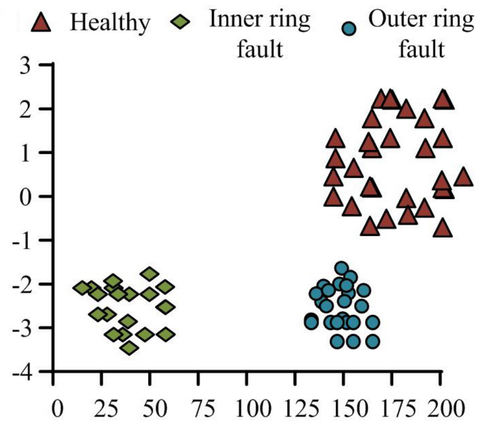

(b) Identify generation domain

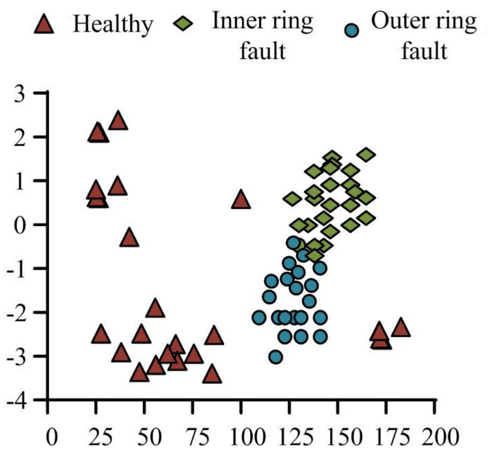

(c) Target domain

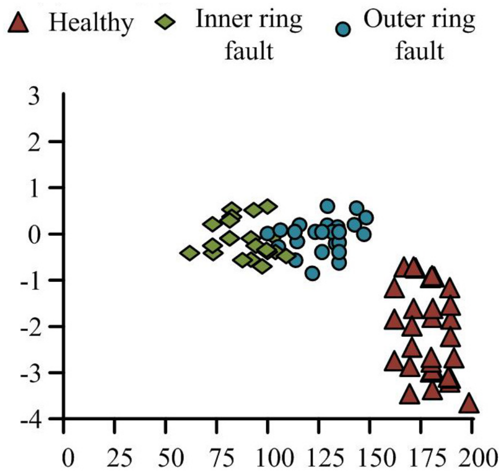

(d) Identify target domain

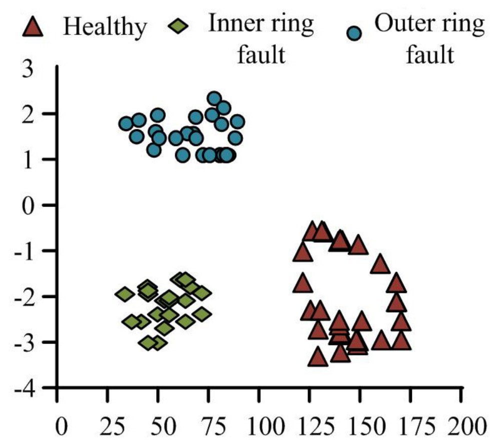

(e) Source domain

FIGURE 12. Visual feature image results generated by the proposed fault diagnosis model

Finally, the robustness of the proposed model is verified by k-fold crossover, and the results are shown in Figure 13.

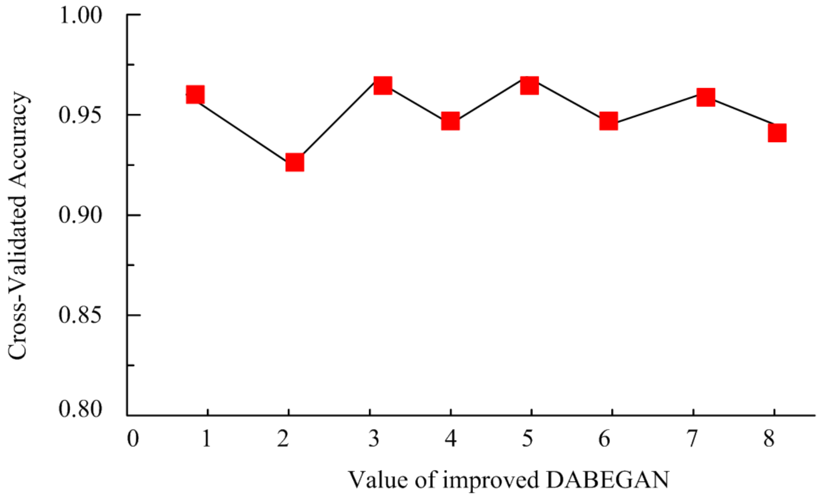

FIGURE 13. Model robustness test

Figure 13 shows the robustness test results of the model. The robustness of the model is discussed through cross validation and analysis of the results of multiple runs of the model. Divide the training set into complementary subsets, train each model with different training subsets, and validate with the remaining validation subsets. Once the model type and hyper parameter are determined, the final model uses these hyper parameters to train on all training sets (i.e., the original training set described above), and the generalization error rate is obtained using the test set. Divide the fault training data into complementary subsets, train each model with different training subsets, and validate with the remaining validation subsets. It can be seen from the above figure that for each super parameter value, 10 fold cross validation is selected, and the hyper parameter values from 1 to 8 are greater than 0.90, indicating that the model has good robustness.

5. **Conclusion.** As an important equipment in industrial automation, motors are widely used in many fields. Once the motor malfunctions, it will inevitably have a serious impact on the production and safety of the enterprise. Traditional motor mechanical fault identification mainly relies on data collection from motor sensors. Due to the complex internal fault factors of the motor, it is difficult to effectively diagnose motor faults. Therefore, based on the improved BGAN network, a BEGAN fault diagnosis model is constructed, and the feature signals collected by the motor physical model are used as training samples to complete mechanical fault diagnosis. Because BEGAN model faces the problem of reducing the correlation between generator input and output data, transfer learning is introduced to build an improved DABEGAN fault diagnosis model and complete the fault case diagnosis test. In the multiple training tests of the proposed fault diagnosis model, the average of the highest diagnostic accuracy of the original BEGAN fault diagnosis model three times is 0.675. Compared with the proposed improved DABEGAN fault diagnosis model, the average diagnostic accuracy of the improved DABEGAN fault diagnosis model exceeded 0.905, which increased by 36.5% compared to the original BEGAN. It can be seen that the improved DABEGAN fault diagnosis model has superior fault diagnosis performance, far higher than the fault diagnosis results of the original BEGAN fault diagnosis model. At the same time, in the fault diagnosis testing of the inner ring of the motor, the proposed fault diagnosis model has a diagnostic accuracy of 0.986, which is superior to the KNN model and K-means model. It can be seen that the proposed fault diagnosis model meets the requirements of modern industrial motor fault diagnosis. There are also shortcomings in research, as the fault characteristics of motors

are complex and more representative fault feature data needs to be extracted to improve the accuracy of fault diagnosis.

Acknowledgement. The research is supported by the Technology Project of State Grid Heilongjiang Electric Power Co., Ltd. (522413220001).

REFERENCES

[1] Y. Li, Y. Song, L. Jia, S. Gao and Q. Li, Intelligent fault diagnosis by fusing domain adversarial training and maximum mean discrepancy via ensemble learning, *IEEE Transactions on Industrial Informatics*, vol.17, no.4, pp.2833-2841, 2020.

[2] Q. Guo, Y. Li, Y. Song and D. Wang, Intelligent fault diagnosis method based on full 1-D convolutional generative adversarial network, *IEEE Transactions on Industrial Informatics*, vol.16, no.3, pp.2044-2053, 2019.

[3] J. Li, R. Huang, G. He, Y. Liao and Z. Wang, A two-stage transfer adversarial network for intelligent fault diagnosis of rotating machinery with multiple new faults, *IEEE/ASME Transactions on Mechatronics*, vol.26, no.3, pp.1591-1601, 2020.

[4] H. Shao, M. Xia, G. Han, Y. Zhang and J. Wan, Intelligent fault diagnosis of rotor-bearing system under varying working conditions with modified transfer convolutional neural network and thermal images, *IEEE Transactions on Industrial Informatics*, vol.17, no.5, pp.3488-3496, 2020.

[5] U. Abubakar, S. Mekhilef, K. S. Gaeid and S. Mokhlis, Induction motor fault detection based on multisensory control and wavelet analysis, *IET Electric Power Applications*, vol.14, no.11, pp.2051-2061, 2020.

[6] Z. Chen, K. Gryllias and W. Li, Intelligent fault diagnosis for rotary machinery using transferable convolutional neural network, *IEEE Transactions on Industrial Informatics*, vol.16, no.1, pp.339-349, 2019.

[7] J. Jiao, M. Zhao and J. Lin, Unsupervised adversarial adaptation network for intelligent fault diagnosis, *IEEE Transactions on Industrial Electronics*, vol.67, no.11, pp.9904-9913, 2019.

[8] H. Shao, M. Xia, J. Wan and W. Clarence, Modified stacked autoencoder using adaptive Morlet wavelet for intelligent fault diagnosis of rotating machinery, *IEEE/ASME Transactions on Mechatronics*, vol.27, no.1, pp.24-33, 2021.

[9] Y. Song, Y. Li, L. Jia and M. Qiu, Retraining strategy-based domain adaption network for intelligent fault diagnosis, *IEEE Transactions on Industrial Informatics*, vol.16, no.9, pp.6163-6171, 2019.

[10] J. Zhang, S. Yi and L. Guo, A new bearing fault diagnosis method based on modified convolutional neural networks, *Chinese Journal of Aeronautics*, vol.33, no.2, pp.439-447, 2020.

[11] R. Liu, F. Wang, B. Yang and S. Qin, Multiscale kernel based residual convolutional neural network for motor fault diagnosis under nonstationary conditions, *IEEE Transactions on Industrial Informatics*, vol.16, no.6, pp.3797-3806, 2019.

[12] H. Tao, P. Wang and Y. Chen, An unsupervised fault diagnosis method for rolling bearing using STFT and generative neural networks, *Journal of the Franklin Institute*, vol.357, no.11, pp.7286-7307, 2020.

[13] M. Zhao, S. Zhong, X. Fu, B. Tang and M. Pecht, Deep residual shrinkage networks for fault diagnosis, *IEEE Transactions on Industrial Informatics*, vol.16, no.7, pp.4681-4690, 2019.

[14] J. Jiao, M. Zhao and J. Lin, Unsupervised adversarial adaptation network for intelligent fault diagnosis, *IEEE Transactions on Industrial Electronics*, vol.67, no.11, pp.9904-9913, 2019.

[15] M. A. S. ALTobi, G. Bevan and P. Wallace, Fault diagnosis of a centrifugal PUMP using MLP-GABP and SVM with CWT, *Engineering Science and Technology, an International Journal*, vol.22, no.3, pp.854-861, 2019.

[16] R. Liu, B. Yang and A. G. Hauptmann, Simultaneous bearing fault recognition and remaining useful life prediction using joint-loss convolutional neural network, *IEEE Transactions on Industrial Informatics*, vol.16, no.1, pp.87-96, 2019.

[17] J. Cen, Z. Yang, X. Liu et al., A review of data-driven machinery fault diagnosis using machine learning algorithms, *Journal of Vibration Engineering & Technologies*, vol.10, no.7, pp.2481-2507, 2022.

[18] Z. Chai and C. Zhao, A fine-grained adversarial network method for cross-domain industrial fault diagnosis, *IEEE Transactions on Automation Science and Engineering*, vol.17, no.3, pp.1432-1442, 2020.

[19] P. Akhenia, K. Bhavsar, J. Panchal and V. Vakharia, Fault severity classification of ball bearing using SinGAN and deep convolutional neural network, *Proceedings of the Institution of Mechanical Engineers, Part C: Journal of Mechanical Engineering Science*, vol.236, no.7, pp.3864-3877, 2022.
[20] S. R. Saufi, Z. A. B. Ahmad, M. S. Leong and M. Lim, Gearbox fault diagnosis using a deep learning model with limited data sample, *IEEE Transactions on Industrial Informatics*, vol.16, no.10, pp.6263-6271, 2020.

Author Biography

Jie Sun received the B.Sc. degree in Computer Science and Technology from Harbin Institute of Technology, China, 2000; the M.Sc. degree in Electrical Engineering from Northeast Electric Power University, China, 2008. Mr. Sun is currently a senior engineer of Qiqihar Power Supply Branch of State Grid Heilongjiang Electric Power Co., Ltd., Qiqihar, China. His research interests include fault line selection. He has published over 15 papers in journals and conferences. He has actively served in a number of journals.

Yan Wang received the B.Sc. degree in Power System and Its Automation from Northeast Electric Power University, China, 1992; the M.Sc. degree in Electrical Engineering from Northeast Electric Power University, China, 2007. Mr. Wang is currently a senior engineer of Qiqihar Power Supply Branch of State Grid Heilongjiang Electric Power Co., Ltd., Qiqihar, China. His research interests include fault line selection and stability control of power system. He has published over 10 papers in journals and conferences. He has actively served in a number of journals.

Yi Sun received the B.Sc. degree in Industrial Automation from Harbin Engineering University, China, 2001; the M.Sc. degree in Electrical Engineering from Northeast Electric Power University, China, 2010. Mr. Sun is currently a senior engineer of Qiqihar Power Supply Branch of State Grid Heilongjiang Electric Power Co., Ltd., Qiqihar, China. His research interests include fault line diagnosis. He has published over 10 papers in journals and conferences. He has actively served in a number of journals.

Fangming Jin received the B.Sc. degree in Computer Science and Technology from Harbin Institute of Technology, China, 2000; the M.Sc. degree in Technology Economy and Management from North China Electric Power University, China, 2008. Mrs. Jin is currently a senior engineer of Qiqihar Power Supply Branch of State Grid Heilongjiang Electric Power Co., Ltd., Qiqihar, China. Her research interests include distribution network fault line selection device. She has published over 10 papers in journals and conferences. She has actively served in a number of journals.